Curcumin Coated Iron-Oxide Nanoparticles: Characterization and Neuroprotective Potential in Parkinson's Disease using a *C. Elegans* Model

Shiven Patel, Umaiyal Nathan, Praneel Shah, Eric Han & Arya Kulkarni

Received June 30, 2024
Accepted October 18, 2024
Electronic access October 31, 2024

Parkinson's disease is a complex and progressive neurodegenerative disorder, affecting over 1,000,000 people in the United States alone. However, iron-oxide nanoparticles have shown promise in treating Parkinson's disease by targeting the ferroptotic pathways associated with iron overload potentially delivering therapeutic agents to the affected brain regions and helping to mitigate some of the debilitating symptoms (motor function loss, cognitive impairment, autonomic dysfunction, etc.) associated with the condition. In this study, iron oxide nanoparticles (INP) were synthesized using cilantro leaf extract (mixed using heat to combine the cilantro with the iron, then decanted cilantro leaves) and ferrous sulfate salt. The synthesized INPs were characterized by Fourier-transform infrared spectroscopy (FTIR), Ultraviolet-visible spectroscopy (UV-Vis), Zetasizer, and X-ray diffraction (XRD) techniques. The potential of INPs for treating neurodegenerative diseases was tested using worm models for Parkinson's disease - Caenorhabditis Elegans (C. Elegans). To ensure minimal toxicity, we conducted additional toxicity assays on all strains using curcumin-coated iron oxide nanoparticles (0.5 mg/ml, 1 mg/ml, 2 mg/ml, and 5 mg/ml). The results suggest that there is significant toxicity when the concentration of INPs is greater than 1 mg/ml concentration, there is also a significant boost in effectiveness and reduction in toxicity when adding curcumin to the nanoparticles. By conducting a Basal Slowing Assay, it was determined that the particles have no negative impact on dopamine signaling in N2 worms, and in mutants with impacted dopamine pathways (dopamine-containing neural circuit that senses a mechanical attribute of bacteria), the particles improved their dopamine signaling.

Introduction

A 2022 Parkinson's Foundation-backed study revealed that nearly 90,000 people are diagnosed with Parkinson's disease in the U.S. each year[1]. This represents a steep 50% increase from the previously estimated rate of 60,000 diagnoses annually[1]. Parkinson's disease is a debilitating neurodegenerative disorder characterized by the progressive loss of dopaminergic neurons in the brain[2]. The hallmark of Parkinson's disease is the specific degeneration of dopaminergic neurons in the substantia nigra pars compacta, leading to reduced dopamine levels in the basal ganglia[2]. Consequently, classical motor symptoms like tremors, bradykinesia, rigidity, and postural instability manifest[2]. Parkinson's disease is also associated with a wide array of non-motor manifestations, including cognitive impairment, sleep disturbances, mood disorders, and autonomic dysfunction[2]. The underlying pathophysiological mechanisms contributing to the development and progression of Parkinson's disease involve a complex interplay of genetic, environmental, and age-related factors[3,4]. Iron is essential in many physiological processes, including DNA metabolism, oxygen transport, and cellular energy generation, which is incredibly important when someone is sick with Parkinson's. Patients with late-stage Parkinson's are also often found to have low iron levels[5].

The Blood blood-brain barrier (BBB) plays a crucial role in safeguarding the central nervous system (CNS) from harmful substances, and its integrity becomes even more significant when considering potential therapeutic interventions for neurological disorders like Parkinson's disease[6]. In recent years, there has been growing interest in utilizing nanoparticles as a novel approach to cross the BBB and deliver drugs to the CNS[7,8].

Nanoparticles owing to their small size and unique properties, offer a promising avenue for targeted drug delivery to the brain[7,9]. Traditional drugs often encounter obstacles in crossing the BBB due to their large molecular size[6]. The blood-brain barrier has a permeability size of 5 to 200 nm. However, when attached to nanoparticles, these drugs can effectively traverse the barrier and gain access to the brain[10]. Among various nanoparticle types, metal nanoparticles have garnered considerable attention for their versatility in shape and size7. They can be engineered to carry drugs and specifically interact with receptors on the exterior surface of the BBB, facilitating their transport into the brain through vesicles[6,11,10]. Moreover, metals themselves play essential roles in various brain functions, such as synaptic plasticity and neurotransmitter production[8].

Despite the potential benefits of nanoparticle-based drug delivery, there are concerns regarding increased BBB permeability, which may lead to the influx of toxic particles and potential damage to neural cells[6]. Thus, researchers are actively exploring safer and more effective methods to achieve drug delivery while maintaining BBB integrity[6].

One such promising avenue involves the use of iron oxide nanoparticles synthesized using cilantro plant extract. Cilantro leaves contain reducing and capping agents that become incorporated into the nanoparticle structure[12]. Furthermore, phytochemicals present in cilantro, such as ketones, aldehydes, flavones, and amides, contribute to its biocompatibility[12,13,14,15]. The incorporation of cilantro leaf extract aims to mitigate the risks associated with increased blood-brain barrier (BBB) permeability and potential neural damage. Cilantro leaf extract, with its natural capping agents and phytochemicals, enhances the stability and biocompatibility of nanoparticles, potentially reducing adverse effects[12]. Iron oxide nanoparticles have shown potential as targeted delivery vehicles for drugs, and the natural elements present in cilantro, such as its nutrient density (vitamin A, vitamin C, vitamin E, and vitamin K), enhance their safety, health benefit, and efficacy[11,10]. Another natural compound of interest is curcumin, derived from turmeric, which has been studied extensively for its anti-cancer properties[16,17]. The use of curcumin-coated nanoparticles is designed to enhance drug delivery across the blood-brain barrier (BBB) while minimizing potential neurotoxic effects, thanks to curcumin's biocompatibility[16,17]. However, its large molecular size limits its cellular uptake and bioavailability[18]. To address this limitation, the use of curcumin-coated nanoparticles to improve its cellular delivery and target specific tissues has been explored[19,20].

In the context of Parkinson's disease, C. Elegans is frequently utilized as a model organism due to its genetic homology to humans and its simple, transparent CNS, allowing for easy visualization under a light microscope[21]. Specifically, the WLZ3 and CB1112 strains were used. The WLZ3 strain has a mutation in the leucine-rich repeat kinase 2 (LRRK2) gene. Mutations in this gene in humans have historically been linked with Parkinson's, making this strain a valuable model to study Parkinson's disease[3]. The CB1112 strain contains a mutation in the cat-2 gene, which codes for tyrosine hydroxylase (TH), and as a result, has lower levels of dopamine. This deficiency is commonly associated with Parkinson's, and thus TH is commonly associated with the development of the disease.

The primary objective of this study is to identify a safe and effective nanoparticle for drug delivery in C. elegans, serving as a model for Parkinson's disease. We aim to evaluate the toxicity and biocompatibility of these nanoparticles to ensure they can deliver therapeutic agents to the brain without causing adverse effects. By assessing the interactions between the nanoparticles and C. elegans, this study seeks to advance the development of targeted drug delivery systems that can be applied during the treatment of Parkinson's disease.

Methods

Strains and Maintenance:

The following Caenorhabditis elegans strains were used in the study: N2 (wild type), WLZ3, and CB1112 (cat-2-defective). All strains were maintained at 16°C on Nematode Growth Medium (NGM) plates seeded with Escherichia coli OP50, following the guidelines outlined in Wormbook. Age synchronizations were performed using a sodium hydroxide and bleach solution, as specified in Wormbook protocols.

Materials

The study utilized curcumin and cilantro extract as chemical reagents and ferrous sulfate (FeSO4) for iron supplementation. A Celestron Digital Microscope Imager was employed for imaging purposes. For sample processing, a centrifuge was used. Detailed structural analysis was conducted using an Amray 1830 Scanning Electron Microscope (SEM) equipped with an energy-dispersive X-ray spectrometer (SEM-EDX). Spectroscopic analysis was performed using a Thermo Scientific Nicolet iS5 Fourier Transform Infrared (FT-IR) Spectrometer. At the same time, absorbance measurements across a range of wavelengths were obtained using a 721 UV-visible-near infrared spectrophotometer. Throughout the assays, analytical grade reagents and deionized water were utilized to ensure the precision and reproducibility of the results.

Fabrication/Characterization of Nanoparticles

Nanoparticle Synthesis

Cilantro leaf extract was prepared by cutting 10 grams of cilantro leaves into small pieces, followed by a thorough washing with deionized water. The washed cilantro leaves were then immersed in 100 ml of deionized water, and the resulting solution was maintained at 15°C for 15 minutes in a fume hood. After cooling to room temperature, the extract was separated from the leaves by passing it through Whatman No. 1 filter paper. The prepared leaf extract was stored in a clean flask at 5°C. Subsequently, 0.01 M FeSO4 in a 100 ml conical flask was prepared, and the cilantro leaf extract was added to this solution with constant agitation using a magnetic stirrer set at 1500 rpm on a hot plate until the solution turned black. The solution was then placed in a water bath maintained at 30°C and stirred slowly with a magnetic stirrer for 15 minutes within a fume hood. The solution was then centrifuged at 3,600 rpm for 20 minutes to obtain a pellet, which was washed with triple distilled water and centrifuged again. Finally, the pellet was freeze-dried at -78°C and 10 Pa pressure for 24 hours.

Curcumin Coating

A 2 mg mL-1 stock solution of curcumin was prepared in acetone. Subsequently, 10 mg of FeSO4 nanoparticles were dissolved in 1 mL of acetone. The curcumin solution was then added to the iron solution. The mixture was then subjected to continuous stirring for 24 hours. The resultant mixture was subjected to centrifugation at 3600 rpm for 20 minutes. The product was washed thrice with distilled water, and centrifuged at 3600 rpm for 20 minutes after each wash, to remove any residual impurities. Finally, the product was frozen in a -80°C freezer[11].

Fourier-Transform Infrared Spectroscopy (FTIR)

Samples of INPs were prepared as thin films, liquid solutions, or powders and placed on suitable holders. The FTIR spectrometer was calibrated, and a background measurement was obtained. Measurements were conducted in attenuated total reflection mode. The obtained spectra were analyzed to identify functional groups and composition using reference databases and software. After each measurement, samples were removed, and equipment was cleaned following manufacturer guidelines. The instrument used was the Thermo Scientific Nicolet iS5 Fourier Transform Infrared (FT-IR) Spectrometer.

Ultraviolet-visible spectroscopy (UV-VIS)

Samples of INPs were prepared in solution form and adjusted to appropriate concentrations. The UV-Vis spectrometer was calibrated using a blank reference solution as the baseline. Measurements were taken within the UV-Vis wavelength range to record absorbance spectra. Quantitative analysis involved measuring absorbance at specific wavelengths and determining sample concentrations using calibration curves from standard solutions. Cleaning procedures were diligently followed after each measurement to prevent contamination.

X-ray diffraction Analysis (XRD)

Samples were prepared as finely ground powders for homogeneity. The X-ray diffractometer was used to obtain diffraction patterns by scanning the samples over a specific angular range[21]. Characteristic peaks were identified to determine the crystal phases present in the sample.

Zeta Potential Characterization

Samples were diluted with DI water using a 10:1 ratio. The resulting solution was added to the Zetasizer's respective cuvette and then added to the Zetasizer. The results were relayed onto the connected computer where characteristic peaks could be observed and analyzed. The cleaning procedure required an intense cleaning process with DI water to ensure no nanoparticles remained in the cuvette.

Lifespan/Toxicity

C. Elegans were age synchronized (halted at the L3 stage) and plated on floxuridine (FUdR) supplemented plates and counted to inhibit reproduction and ensure accuracy in worm counts. Each plate had approximately 10 worms before experimentation. They were then exposed to varying concentrations (0.5 mg/ml, 1 mg/ml, 2 mg/ml, 5 mg/ml) of nanoparticles and deionized water. The plates were then checked after 48 hours to count the number of C. Elegans displaying signs of life.

Basal Slowing:

Approximately 100 worms of each strain (well-fed age-synchronized L4 stage worms) were rinsed with M9 buffer to eliminate residual bacteria, then centrifuged at 2000 RPM for 2 minutes to remove the excess M9, and split into 4 even groups. A quarter of the worms were transferred to an NGM plate seeded with OP50, another quarter to an NGM plate seeded with INPs, another quarter to an NGM plate seeded with both OP50 and INPs, and the final quarter to an NGM plate coated with M9 buffer (as a control). The concentration of INPs used was 1mg/mL, as this was found to be the most promising in the toxicity assays. After 2 minutes of acclimatization, sections of the plates were recorded for 45 seconds using the Celestron Microscope Imager. The videos were processed by visual counting of body bends/minute by multiple researchers.

Results

Characterizations

UV-Vis Characterization:

Ultraviolet-visible spectroscopy is utilized to confirm that the nanoparticle samples synthesized are truly Iron Sulphate nanoparticles. If the absorbance peaks through our experimentation match existing literature of Iron Sulphate nanoparticles, then we can conclude we successfully synthesized the nanoparticles.

FTIR Characterization

The primary objective of Fourier Transform Infrared Spectroscopy (FTIR) is to identify the presence of curcumin within the iron nanoparticle sample. If curcumin is properly loaded onto the nanoparticle surface, it will display a distinct absorbance peak that won't be present in the control sample.

Iron Nanoparticles:

FT-IR analysis of iron metal nanoparticles revealed peak absorbances at 593.30 cm-1, 1633.63 cm-1, 1096.43 cm-1, and 3329.73 cm-1. These peaks signify the vibration of Fe-O bonds, stretching vibration of acyclic C-C bonds, symmetric C-O vibration associated with the C-O-SO3 group, and OH stretching of water molecules, respectively.

Curcumin Coated Nanoparticles:

FT-IR analysis of curcumin-coated iron metal nanoparticles revealed peak absorbances at 578.63 cm^{-1}, 597.40 cm^{-1}, 1635.27 cm^{-1}, 2012.31 cm^{-1}, 2158.04 cm^{-1}, and 3320.46 cm^{-1}. These peaks signify the vibration of Fe-O bonds, the stretching vibration of C=O bonds in curcumin, the potential presence of CN or other functional groups, the potential presence of C-H or other functional groups, and OH stretching

Figure 1: Diagrams of Nanoparticle Synthesis

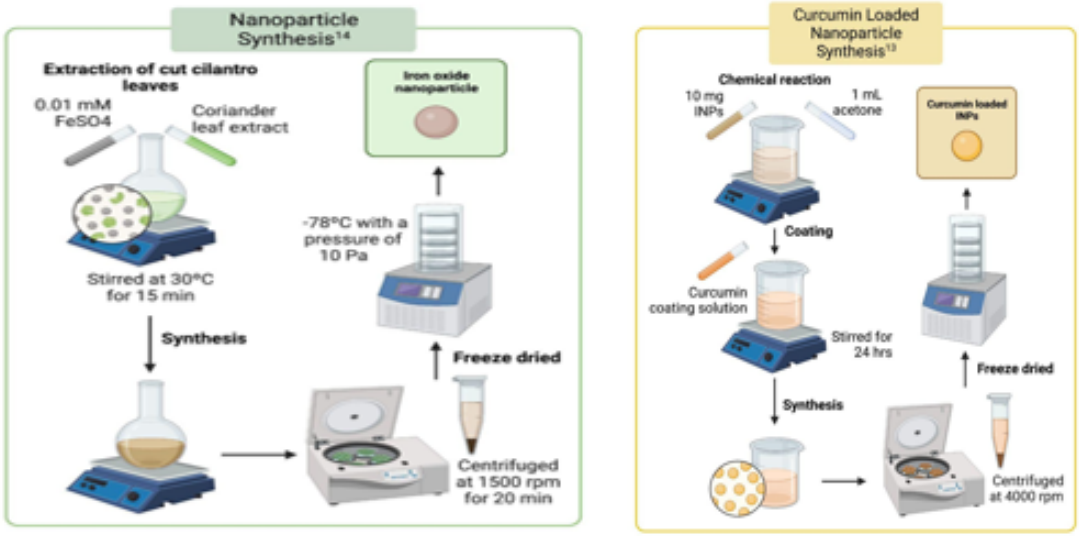

Sub figure 1a, 1b: Iron nanoparticle synthesis, curcumin coating of iron nanoparticles

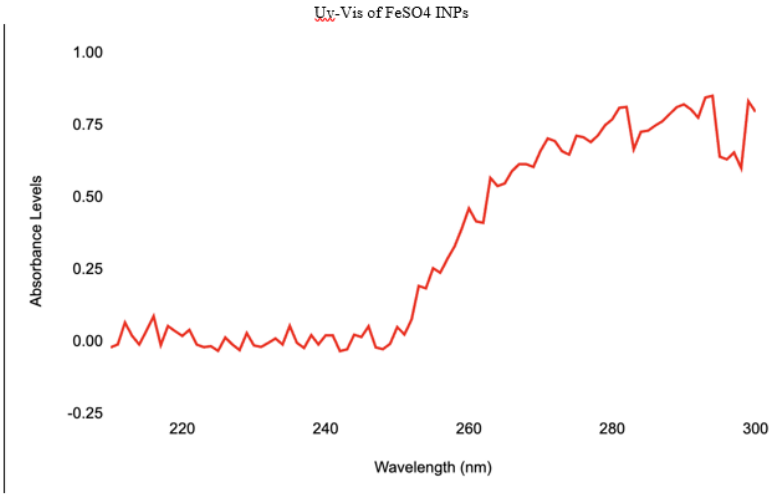

UV-VIS for Iron Oxide showed a peak at 294 nm which is similar to the reference article[22].

vibrations of water molecules or hydroxyl groups. The presence of curcumin can be seen through the peak of 2012.31 cm^{-1}. The peak at 2012.31 cm^{-1} signifies the robust presence of C-H stretching vibrations, likely originating from aromatic rings or aliphatic groups in curcumin[23].

XRD Characterization

X-ray diffraction tests are conducted to provide comprehensive information about crystalline structure and phase identification. This data will be used to assess the materials' properties and behavior, which can impact its performance in drug delivery applications.

The XRD patterns were compared with the standard Joint Committee on Powder Diffraction Standards (JCPDS) to confirm the crystal structure and phase identification. The XRD of Iron oxide produced a faint signal identical to the ones tested in reference[24]. The XRD confirms that the INPs have a crystalline structure with its sharp peaks instead of broadly humped peaks There was a strong diffraction peak with a 2θ

Figure 2: FTIR Data for Nanoparticles

Iron Nanoparticles	Curcumin Coated Nanoparticles
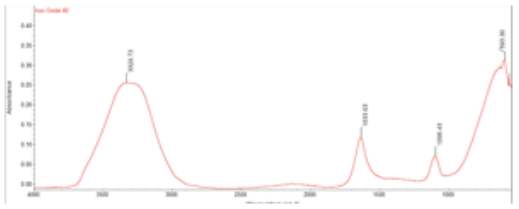	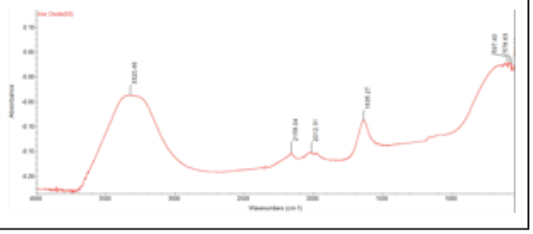

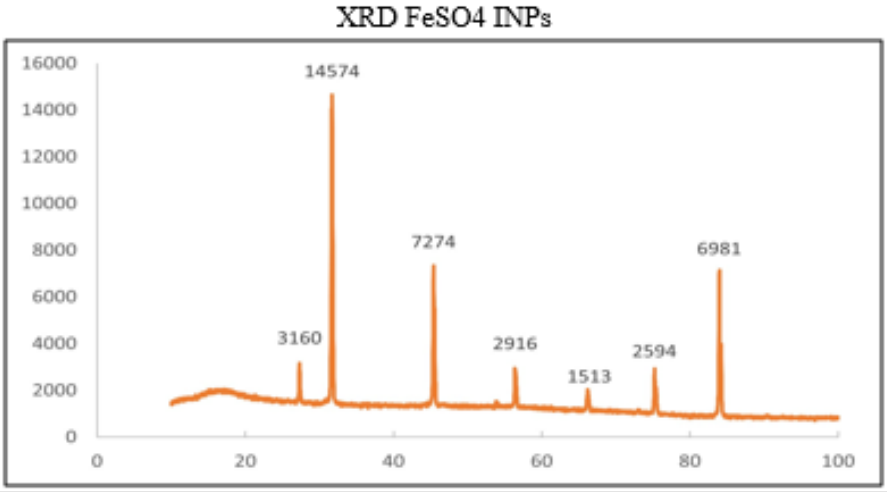

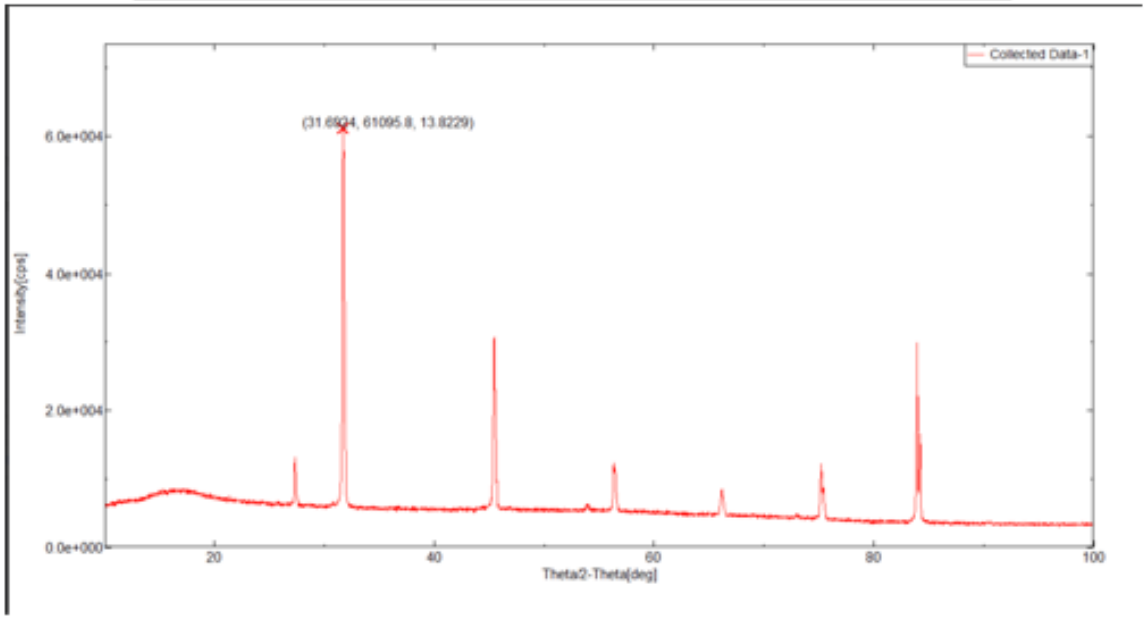

value of 31.6°. The Scherrer equation relates peak broadening in XRD patterns to smaller crystallite sizes; narrower peaks indicate larger crystals. Using the highest peak of 14574 and the Scherrer Formula, the size of the crystallite is 42.75 nm where

K is 0.94, Cu Kalpha is 1.75 angstroms, 2θ is 31.6°, and the β is 0.004. The crystalline size was in the same range as the reference paper[24].

SEM Characterization

Scanning Electron Microscopy was utilized to get a visual on the nanoparticle sample on a nanoscale level. This was performed to identify the size of both INPs and Curumin-Coated INPs.

Zeta Potential Characterization

Zeta Characterization was used to better understand the chemical properties present within the INPs.

The curcumin nanoparticles exhibit an average zeta potential of -19.267, indicating their predominantly anionic character. This anionic property renders them particularly effective in their role as corrosion inhibitors as they can readily adsorb onto positively charged metal surfaces, forming a protective layer that prevents oxidation and corrosion[25]. Zeta potential not only informs us about the stability and charge characteristics of the nanoparticles but also highlights their suitability for applications in corrosion protection.

Assays

Dopamine-related behaviors like Basal Slowing Response (BSR) are a way of further assessing the Curcumin-coated INPs. As such, a Basal Slowing Assay was performed on N2 (control) and CB1112 (dopamine defective) strains both with and without exposure to the nanoparticles. The Basal Slowing Assay tests the worms' behavior when in the presence or absence of food (bacterial) on agar plates. Since the N2 worms have intact dopamine signaling pathways, as expected, their motion was greater in the plates without food than in the plates with food[26]. There was also no significant difference in BSR between the control and INP groups, demonstrating that the nanoparticles are not negatively influencing dopamine-dependent behaviors such as BSR. In the CB112 worms, there was no difference between the plates with food and without food, because of their impacted dopamine signaling. However, in the INP group, there was an increase in BSR.

Survival rates were compared across different concentrations using one-way ANOVA26, followed by Tukey's post-hoc test. Significant differences were observed between the 0.5 mg/ml and 5 mg/ml groups ($p < 0.05$), with the survival rates at 0.5 mg/ml and 1 mg/ml concentrations being significantly higher compared to the 5 mg/ml concentration. Replication experiments were conducted to ensure reliability, with standard deviations provided as 5.24%, 3.12%, 6.73%, and 1.89%, respectively.

Discussion

In the characterization of the iron oxide nanoparticles (INPs), the X-ray diffraction (XRD) analysis indicated a well-defined crystalline structure with an average size of 42.75 nm, as determined by the Scherrer Formula, with the highest peak at 14574. These findings align closely with previous studies utilizing Cu Kalpha (1.75 angstroms, 2θ 31.6°, β 0.004), lending credibility to our measurements and ensuring the consistency of our results. All the peaks of XRD confirm the presence of only INPs and no significant impurities[11]. Scanning Electron Microscopy (SEM) revealed a particle size of 68 nm along with clusters of particles up to 192 nm for both curcumin and plain iron nanoparticles. The curcumin nanoparticles also had zeta potential that averaged to -19.267, establishing the particles as anionic making them corrosive inhibiting in nature.

In the toxicity assay, we conducted experiments on C. Elegans exposed to four different concentrations of INPs dissolved in DI water: 0.5 mg, 1 mg, 2 mg, and 5 mg/ml. Our decision to use DI water as a solvent was well-founded, as it was found to be less toxic to the worms compared to ethanol, ensuring that the observed effects were predominantly attributed to the INPs. After 48 hours of exposure, we assessed the survival rate of the wild-type (N2) worms, which showed values of 58.84%, 72.32%, 33.33%, and 0% at the respective concentrations.

Similarly, for the WLZ3 strain, the survival rates were 31%, 29%, 11%, and 0%, respectively. Our results demonstrate significant toxicity beginning at 1 mg/ml, with the WLZ3 strain exhibiting a more pronounced sensitivity to the nanoparticles. To explore potential solutions to mitigate toxicity, we conducted additional toxicity assays on the WLZ3 strain using curcumin-coated iron nanoparticles. The results were promising, with survival rates of 70%, 88%, 74%, and 13% at the same respective concentrations, while toxicity assays carried out on N2 worms with the curcumin-coated iron nanoparticles resulted in lower survival rates compared to WLZ3, being 70.67%, 81%, 52.10%, and 19.67% at the same respective concentrations.

This suggests that the curcumin coating on iron nanoparticles could play a crucial role in reducing toxicity, especially in worms representing Parkinson's disease as shown by them having a higher overall survival rate with curcumin compared to N2[9]. Given that curcumin is recognized for its anti-inflammatory and antioxidant properties, it is likely to aid in counteracting the negative effects of iron overload in C. elegans and may hold promise for applications in human medicine.

Cat-2 mutated worms do not carry the genes that produce tyrosine, a precursor to dopamine[22]. As a result, their dopamine pathways are impacted by an inability to synthesize dopamine. However, our results have shown that when exposed to curcumin-coated INPs, these mutants exhibit an improvement in dopamine-related behavior, mainly BSR. The synergistic effects of curcumin-coated INPs might reduce oxidative stress and enhance cellular resilience, compensating for the lack of dopamine production in Cat-2 mutants and improving behavioral outcomes and survival rates.

Overall, the study's findings strongly support the potential of curcumin-coated INPs as a strategy for reducing toxicity in drug

Figure 3: Zeta potential of Curcumin Coated INPs

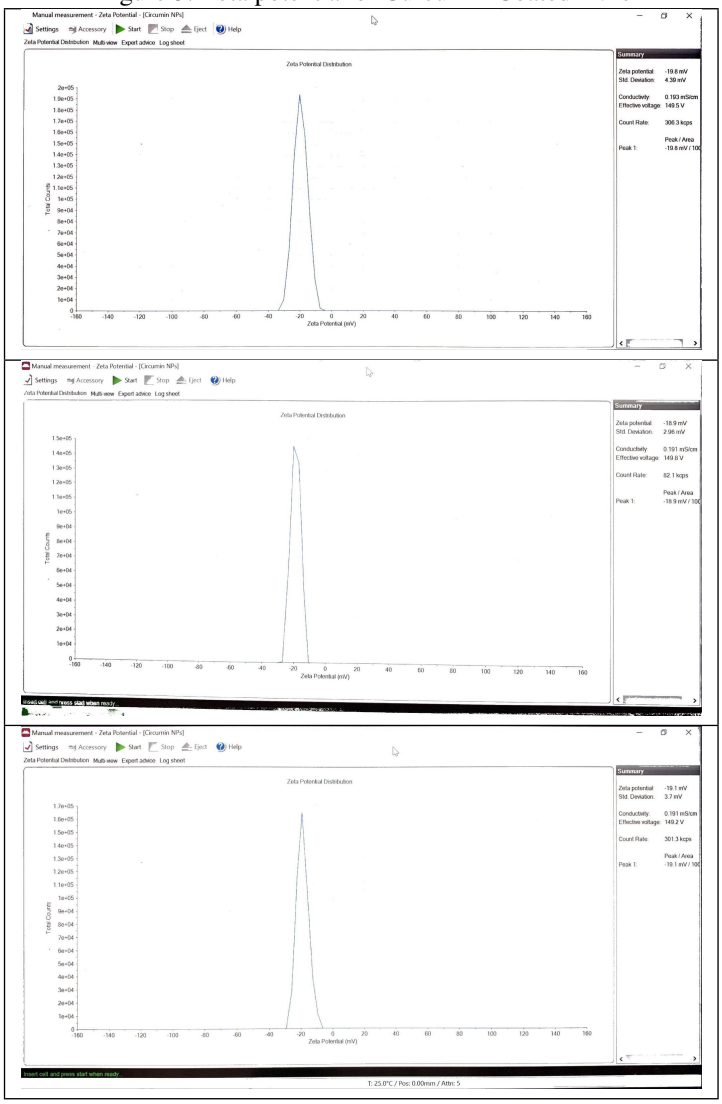

Figure 4: Basal Slowing Curcumin coated Iron Nanoparticles

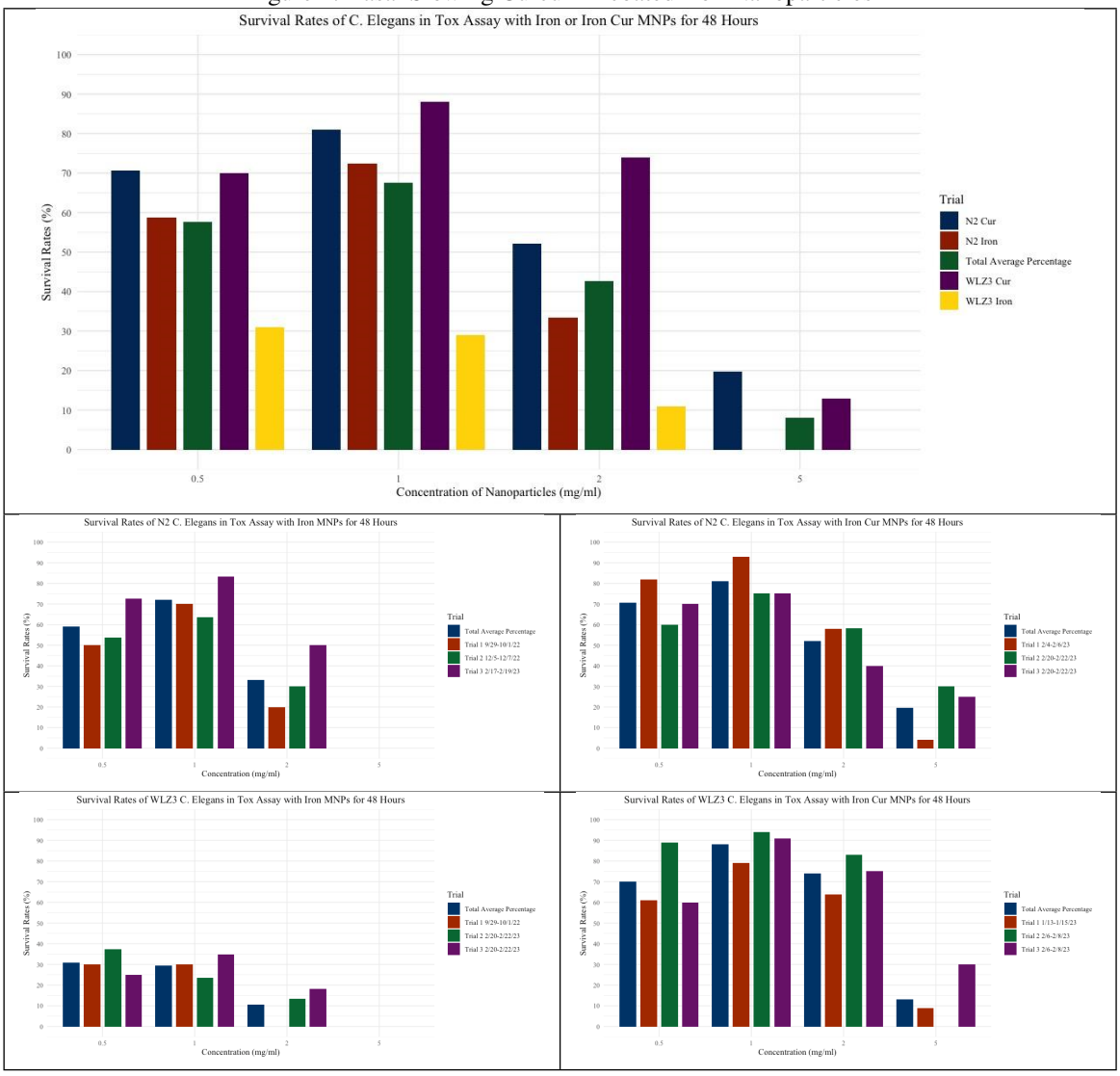

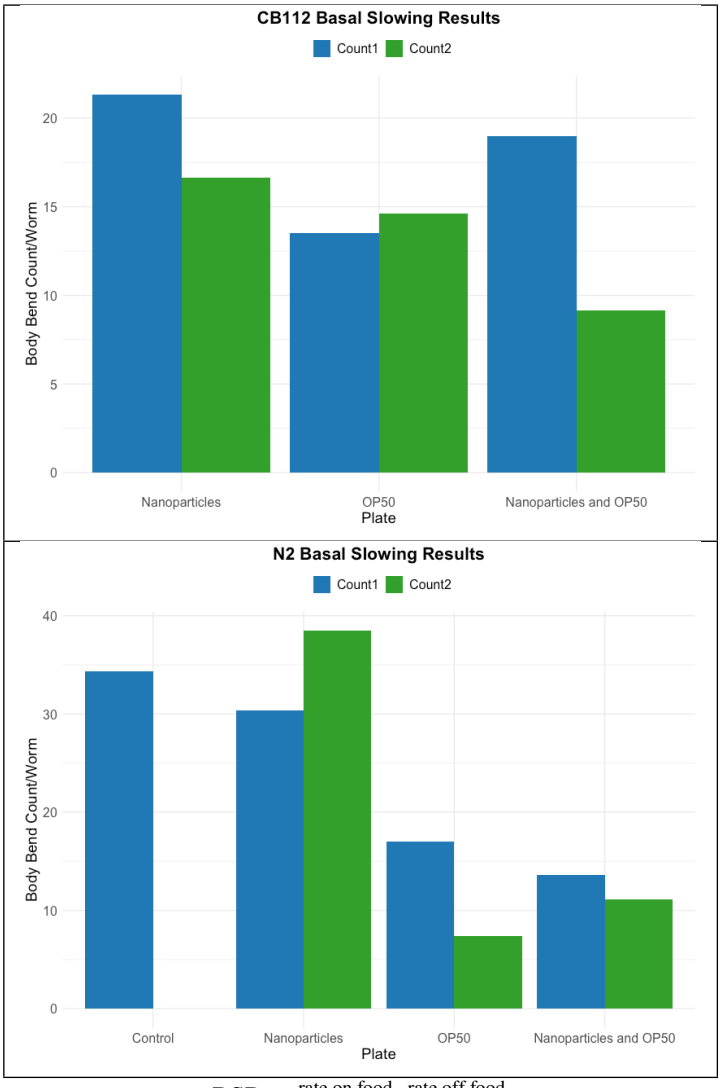

$$\text{BSR} = \frac{\text{rate on food} - \text{rate off food}}{\text{rate off food}}$$

Figure 2: SEM Images of INPs

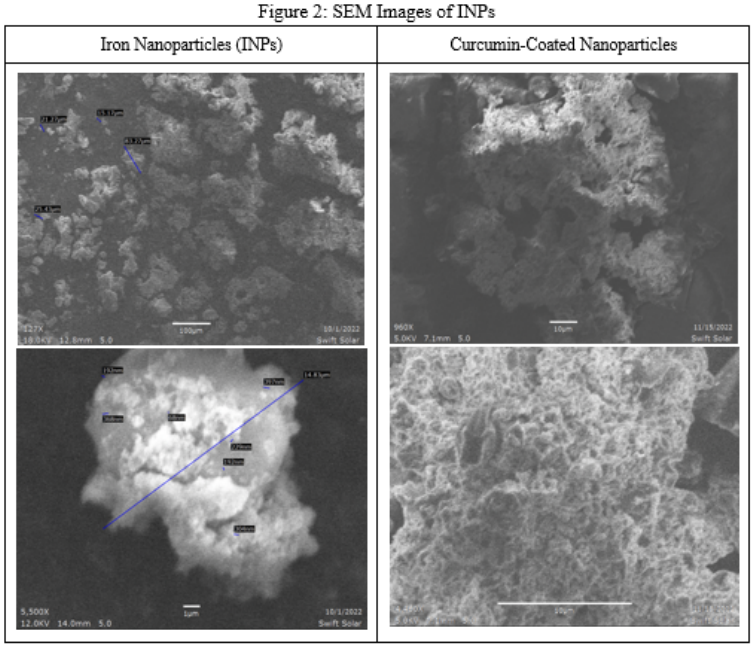

The particles had an average size of 68 nm along with clusters of particles up to 192 nm.

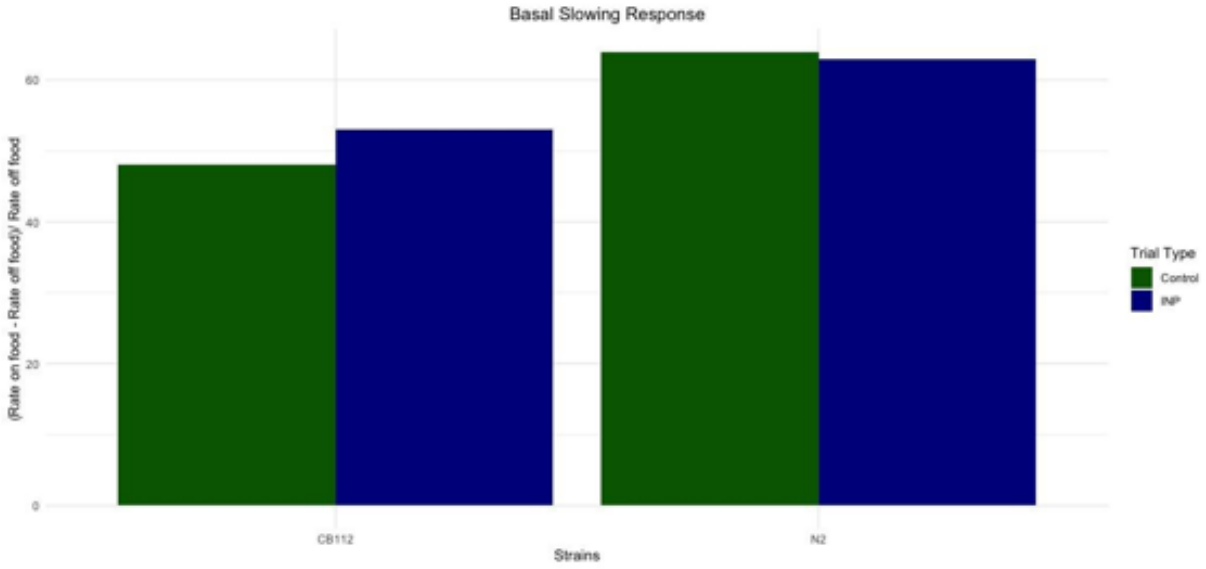

delivery systems. However, to optimize their efficacy, additional research is needed to precisely determine the ideal concentration of curcumin and iron in these nanoparticles. It is crucial to highlight that concentrations above 1 mg/ml of all particle types and strains have shown notable toxicity, emphasizing the necessity for meticulous dosage considerations in potential medical applications [19]. Further advancements in this direction hold the key to safer and more effective drug delivery systems.

Future Scope

Advancing towards clinical applications, the research on curcumin-coated iron nanoparticles aims to forge a path towards clinical applications, necessitating thorough investigation in several key areas. Initially, we must elucidate curcumin's protective mechanisms through studies on signaling pathways, gene expression, and cellular responses in both C. Elegans and mammalian cell cultures. This will be complemented by exploring the interactions between curcumin, iron nanoparticles, and biological environments to understand stability, release kinetics, and intracellular behavior.

The transition to in vivo validation is crucial, where rodent and non-human primate studies will provide insights into safety, efficacy, and mammalian system responses, including biodistribution and pharmacokinetics. These findings are vital precursors to human clinical trials. Human trials, particularly with conditions like Parkinson's disease or iron overload, will also focus on safety, efficacy, and pharmacokinetics. It is critical to monitor dosing, side effects, and therapeutic efficacy closely.

We also aim to enhance therapeutic potential through targeted delivery, investigating nanoparticles functionalized with specific ligands or antibodies to optimize site-specific accumulation and reduce off-target effects. This approach may lower dosage requirements and minimize toxicity. Assessing long-term safety through chronic exposure studies in relevant animal models is imperative to understand cumulative effects and ensure safety during prolonged administration.

Lastly, optimizing nanoparticle manufacturing for clinical application is essential. We will focus on consistent quality, scalable production, and adherence to regulatory standards like Good Manufacturing Practices (GMP) to ensure safety and efficacy for human use.

Conclusion

This research underscores the potential of iron oxide nanoparticles (INPs) created using cilantro leaf extract as an innovative method for treating Parkinson's disease. Our study using these nanoparticles in C. Elegans models of Parkinson's disease reveals encouraging prospects for their therapeutic use. Their ability to penetrate the blood-brain barrier (BBB) marks a notable advancement in treatments for neurodegenerative diseases.

In experiments with the WLZ3 and CB1112 strains of C. Elegans, INPs significantly reduced Parkinson's disease symptoms, proving their effectiveness in targeting the brain areas impacted by the disease. However, the toxicity observed at concentrations over 1 mg/ml highlights the importance of precise dosage control. Notably, coating these nanoparticles with curcumin both increased their efficacy and markedly decreased toxicity, illustrating the combined potential of natural substances and nanotechnology. Our findings suggest that INPs are a promising treatment for Parkinson's disease, but require careful optimization to balance therapeutic effects with minimal side effects. The innovative use of cilantro leaf extract and curcumin to create these nanoparticles introduces a natural and biocompatible approach, which could lead to more effective and safer treatments for neurodegenerative diseases.

Future studies should delve into the detailed mechanisms of how INPs deliver their therapeutic impact and the long-term effects of their usage. Broadening this research to include mammalian models and eventually clinical trials is essential for turning these discoveries into viable treatments for Parkinson's disease.

Acknowledgements

Conflict of Interest
We thank the Aspiring Scholars Directed Research Program (ASDRP) for providing the resources and support necessary for this research. The facilities and assistance provided were integral to the successful completion of our project. We would also like to thank the Caenorhabditis Genetics Center (CGC) for supplying the C. elegans strains used in this study. Their contribution was vital to our research. The authors declare no conflict of interest

Contributions
Gayathri Renganathan (GR) and Neelima Sangeneni (NS) conceptualized this research project. Shiven Patel (SP)managed research task distribution, assisted with the basal slowing assay, conducted toxicity assays, and completed FTIR, Zeta, and UV-Vis characterizations for both sets of particles. SP also aided in synthesizing particles, modeled data in R for graphs, and contributed to the general management of C. elegans, as well as writing parts of the manuscript. Praneel Shah (PS) assisted with FTIR, Zeta, and UV-Vis characterizations, led the synthesis of nanoparticles, helped analyze data for the basal slowing assay, and worked on the general management of C. Elegans. PS also wrote parts of the manuscript. Umaiyal Nathan (UN) led the basal slowing assay, led the general management of C. elegans, and wrote parts of the manuscript. Eric Han (EH) assisted with toxicity assays and the general management of C. Elegans. Arya Kulkarni (AK) performed SEM imaging for nanoparticles.

References

1 C. Marras, J. C. Beck, J. H. Bower, E. Roberts, B. Ritz, G. W. Ross, R. D. Abbott, R. Savica, S. K. Van Den Eeden, A. W. Willis and C. M. Tanner, *Npj Parkinson's Disease*, 2018, **4**, 1–7.

2 M. Maulik, S. Mitra, A. Bult-Ito, B. E. Taylor and E. M. Vayndorf, *Frontiers*, 2017.

3 M. F. for Medical Education and Research, *Parkinson's Disease*, https://www.mayoclinic.org/diseases-conditions/

parkinsons-disease/symptoms-causes/syc-20376055, 2022.

4 J. H. Kim, J. K. Oh, J. H. Wee, C. Y. Min, D. M. Yoo and H. G. Choi, *Brain sciences*, 2021, **11**, 623.

5 ScienceDaily, *Nanomaterials shape and form influence their ability to cross the Blood-Brain Barrier*, https://www.sciencedaily.com/releases/2021/07/210705152052.htm, 2021, Retrieved May 18, 2022.

6 A. Bu, *What Is Iron Oxide? Iron oxide nanoparticles, characteristics, and applications*, https://www.sigmaaldrich.com/US/en/technical-documents/technical-article/materials-science-and-engineering/biosensors-and-imaging/iron-oxide-nanoparticles-characteristics-and-applications, Retrieved May 19, 2022.

7 A. C. V. De Guzman *et al.*, *Nanomaterials*, 2022, **12**, 758.

8 N. Carter, *Physical Properties of Iron Oxide Nanoparticles*, Honors College. 210. Retrieved from https://digitalcommons.library.umaine.edu/honors/210, 2015.

9 L. B. Thomsen, M. S. Thomsen and T. Moos, *Therapeutic delivery*, 2015, **6**, 1145–1155.

10 K. Singh, D. S. Chopra, D. Singh and N. Singh, *Arabian Journal of Chemistry*, 2020.

11 A. C. V. De Guzman, A. Razzak, J. H. Cho, J. Y. Kim and S. S. Choi, *Nanomaterials*, 2022, **12**, 758.

12 R. Link, *The herb that benefits the heart, Brain & Heart*, https://draxe.com/nutrition/cilantro-benefits/, 2021, Retrieved May 19, 2022.

13 Preetidubey, *Properties of coriander or cilantro (Coriandrum sativum)*, https://themodernvedic.com/herbs-natural-foods/properties-coriander-cilantro/, 2018, Retrieved May 19, 2022.

14 Y. Su, W.-Y. Hsu, T.-S. Huang and A. Simonne, *Horticulturae*, 2021, **7**, 122.

15 S. J. Hewlings and D. S. Kalman, *Foods (Basel, Switzerland)*, 2017, **6**, 92.

16 S. Hu, P. Maiti, Q. Ma, X. Zuo, M. R. Jones, G. M. Cole and S. A. Frautschy, *Expert review of neurotherapeutics*, 2015, **15**, 629–637.

17 A. Karthikeyan, N. Senthil and T. Min, *Frontiers in Pharmacology*, 2020, **11**, 487.

18 R. Bhandari, P. Gupta, T. Dziubla and J. Z. Hilt, *Materials Science and Engineering: C*, 2016, **67**, 59–64.

19 D. Patra and R. El Kurdi, *Green Chemistry Letters and Reviews*, 2021, **14**, 474–487.

20 A. Laromaine, *Advances in Colloid and Interface Science*, 2021.

21 YouTube, *C. Elegans N2 Wildtype*, https://www.youtube.com/watch?v=AiO8xsjAtv8, 2020.

22 V. A. Niraimathee, V. Subha, E. Ravindran and S. Renganathan, *International Journal of Environment and Sustainable Development*, 2016, **15**, 227.

23 N. C. for Biotechnology Information, *PubChem Compound Summary for CID 969516, Curcumin*, https://pubchem.ncbi.nlm.nih.gov/compound/Curcumin, 2023, Retrieved November 5, 2023.

24 M. Ma, Y. Wu, J. Zhou, Y. Sun, Y. Zhang and N. Gu, *Journal of Magnetism and Magnetic Materials*, 2004, **268**, 33–39.

25 G. V. Lowry, R. J. Hill, S. Harper, A. F. Rawle, C. O. Hendren, F. Klaessig and J. Rumble, *Environmental Science: Nano*, 2016, **3**, 953–965.

26 E. Sawin, *Neuron*, 2000, **26**, 587–596.

Appendix

Sources Consulted

1. Balasubramanian, C., Joseph, B., Gupta, P., Saini, N. L., Mukherjee, S., di Gioacchino, D. D. G., & Marcelli, A. (n.d.). X-ray absorption spectroscopy characterization of iron-oxide nanoparticles synthesized by high-temperature plasma processing. Retrieved from https://arxiv.org/pdf/1401.3655.pdf
2. Batool, S., Khera, R. A., Hanif, M. A., & Ayub, M. A. (2020). Bay Leaf. Medicinal Plants of South Asia. Retrieved May 19, 2022, from https://www.ncbi.nlm.nih.gov/pmc/articles/PMC7152419/
3. Buchman, J. T., Hudson-Smith, N. V., Landy, K. M., & Haynes, C. L. (2019). Understanding nanoparticle toxicity mechanisms to inform redesign strategies to reduce environmental impact. Accounts of Chemical Research, 52(6), 1632–1642. https://doi.org/10.1021/acs.accounts.9b00053
4. Cooper, J. F., & Van Raamsdonk, J. M. (2018). Modeling Parkinson's Disease in C. elegans. Journal of Parkinson's Disease. https://www.ncbi.nlm.nih.gov/pmc/articles/PMC5836411/ref049
5. Cooper, J.F., Machiela, E., Dues, D.J. et al. Activation of the mitochondrial unfolded protein response promotes longevity and dopamine neuron survival in Parkinson's disease models. Sci Rep 7, 16441 (2017). https://doi.org/10.1038/s41598-017-16637-2
6. Darwesh, R., & Elbialy, N. S. (2021). Iron oxide nanoparticles conjugated curcumin to promote high therapeutic efficacy of curcumin against hepatocellular carcinoma. Inorganic Chemistry Communications, 126, 108482.
7. Fakhari, S., Jamzad, M., & Kabiri Fard, H. (2019). Green synthesis of zinc oxide nanoparticles: A comparison. Green Chemistry Letters and Reviews, 12(1), 19–24. https://doi.org/10.1080/17518253.2018.1547925
8. Gaigneaux, E., De Vos, D. E., Jacobs, P. A., Martens, J. A., Ruiz, P., Poncelet, G., & Grange, P. (2002). Scientific bases for the preparation of heterogeneous catalysts. Elsevier.
9. Jesus, M. B. de. (2019, May 23). Nanomaterials in the Environment: Perspectives on in vivo Terrestrial Toxicity Testing. Frontiers in Environmental Science. https://www.academia.edu/39236635/Nanomaterials_in_the_Environment_Perspectives_on_in_Vivo_Terrestrial_Toxicity_Testing?email_work_card=thumbnail
10. Ke, T., Santamaría, A., Tinkov, A. A., Bornhorst, J., & Aschner, M. (2020). Generating Bacterial Foods in Toxicology Studies with Caenorhabditis elegans. Current protocols in toxicology, 84(1), e94. https://doi.org/10.1002/cptx.94
11. Luo, S., Ma, C., Zhu, M. Q., Ju, W. N., Yang, Y., & Wang, X. (2020). Application of Iron Oxide Nanoparticles in the Diagnosis and Treatment of Neurodegenerative Diseases With Emphasis on Alzheimer's Disease. Frontiers in cellular neuroscience, 14, 21. https://doi.org/10.3389/fncel.2020.00021
12. Perera, W. P. T. D., Dissanayake, R. K., Ranatunga, U. I., Hettiarachchi, N. M., Perera, K. D. C., Unagolla, J. M., ... & Pahalagedara, L. R. (2020). Curcumin loaded zinc oxide nanoparticles for activity-enhanced antibacterial and anticancer applications. RSC advances, 10(51), 30785-30795. https://pubs.rsc.org/en/content/articlelanding/2020/ra/d0ra05755j
13. Roy, A., Singh, V., Sharma, S., Ali, D., Azad, A. K., Kumar, G., & Emran, T. B. (2022). Antibacterial and Dye Degradation Activity of Green Synthesized Iron Nanoparticles. Journal of Nanomaterials, 2022, Article ID 3636481, 6 pages. https://doi.org/10.1155/2022/3636481
14. Stiernagle, Theresa Maintenance of C. elegans. The C. elegans Research Community WormBook WormBook February 11, 2006 1551-850710.1895/wormbook.1.101.1 http://www.wormbook.org
15. Sutphin, G. L., & Kaeberlein, M. (2009, May 12). Measuring Caenorhabditis elegans lifespan on solid media. Journal of Visualized Experiments: JoVE. https://www.ncbi.nlm.nih.gov/pmc/articles/PMC2794294/
16. Tsai, M. H., Chao, H. R., Jiang, J. J., Su, Y. H., Cortez, M. P., Tayo, L. L., Lu, I. C., Hsieh, H., Lin, C. C., Lin, S. L., Wan Mansor, W. N., Su, C. K., Huang, S. T., Hsu, W. L. (2021). Toxicity of Low-dose Graphene Oxide Nanoparticles in an in-vivo Wild Type of Caenorhabditis elegans Model. Aerosol Air Qual. Res. 21, 200559. https://doi.org/10.4209/aaqr.200559
17. U.S. Department of Health and Human Services. (2020, March 3). Test distinguishes Parkinson's disease from related condition. National Institutes of Health. https://www.nih.gov/news-events/nih-research-matters/test-distinguishes-parkinsons-disease-related-condition
18. Verma, A. D., Jain, N., Singha, S. K., Quraishi, M. A., & Sinha, I. (2016). Green synthesis and catalytic application of curcumin stabilized silver nanoparticles. Journal of Chemical Sciences, 128, 1871-1878.
19. Vijayakumar, S., Vaseeharan, B., Malaikozhundan, B., & Shobiya, M. (2016). Laurus nobilis leaf extract mediated green synthesis of ZnO nanoparticles: Characterization and Biomedical Applications. Biomedicine & Pharmacotherapy, 84, 1213–1222. https://doi.org/10.1016/j.biopha.2016.10.038
20. Wang, S., Su, R., Nie, S., Sun, M., Zhang, J., Wu, D., & Moustaid-Moussa, N. (2014). Application of nanotechnology in improving bioavailability and bioactivity of diet-derived phytochemicals. The Journal of nutritional biochemistry, 25(4), 363–376. https://doi.org/10.1016/j.jnutbio.2013.10.002